Generation of the Photoacoustic Effect through Heat Diffusion: Transient Grating Measurements in Reverse Micellar Solutions

Y. N. Cao, H. X. Chen, G. J. Diebold,* T. Sun,† and M. B. Zimmt

Department of Chemistry, Brown University, Providence, Rhode Island 02912

Received: November 18, 1996; In Final Form: January 29, 1997[⊗]

We report the application of the transient grating method to measurement of radii of inverse micelles. A theoretical model is used to calculate the time evolution of the grating as a function of the solution thermal properties and the radii of the micelles. The method is based on the large difference in the thermal expansion coefficients between water and organic solvents: energy deposited in the aqueous interior of the micelles by the optical exciting beams does not result in sizeable photoacoustic effect until heat diffuses into the surrounding organic solvent. The time profile of the transient grating signal is shown to be a function of the micellar radius, and the thermal conductivity and thermal diffusivity of the aqueous and organic subphases. For water-in-alkane reverse micelles, heat deposition is limited to the aqueous interior of the micelles through the use of ionic dyes. Experiments are reported using 1−3 GHz acoustic waves in solutions containing micelles with diameters in the range 10−30 nm. The correspondence between radii determined by the thermal diffusion method and those from dynamic light scattering measurements is discussed.

Introduction

When an optically thin body is irradiated by light, the role of heat diffusion in the production of the photoacoustic effect[1−8] is determined by the ratio of the thermal diffusion time to the transit time of sound across the body or, equivalently, by the ratio of the heat conduction length to the dimensions of the body.[9] When this ratio is small, changes in the dimensions of the irradiated body from heat conduction are considered to be inconsequential during the time the sound wave is launched so that description of the photoacoustic effect reduces to determining the effect of a uniform mechanical motion of the body. In practice, calculation of the waveform from the irradiated body becomes greatly simplified in this case since the coupled equations for the pressure and temperature that govern the photoacoustic effect reduce to a single wave equation for the pressure with a source term describing the volume change from thermal expansion of the body.[10] At the opposite extreme, when heat conduction cannot be ignored, the dimensions of the body change as a result of heat conduction at the same time the sound wave is launched. Determination of the properties of the photoacoustic effect then becomes difficult since immediately after the absorption of radiation heat conduction at the boundary of the body normally results in a localized cooling and hence a contraction of the irradiated body, while at the same time the heat diffusion into the surrounding medium from thermal conduction causes the medium to expand. Despite the wealth of thermal and acoustic information that could be gleaned from the recording of a photoacoustic waveform from a single particle whose dimensions are such that heat conduction influences the characteristics of the photoacoustic effect, little interest in the properties of the photoacoustic effect in the small particle limit has been generated since the demands put on both the time resolution of the acoustic recording apparatus and its detection sensitivity are patently excessive.

In this paper, generation of the photoacoustic effect by heat diffusion from small diameter water droplets into a surrounding organic liquid is discussed. The experimental problem of obtaining sufficient sensitivity is approached by using a "water-in-oil", reverse micellar solution so that a large number of droplets generate the photoacoustic effect. The solution contains an ionic dye soluble in the aqueous interior of the micelles but not in the surrounding hydrocarbon. Since the solvent used here, isooctane, is transparent at the wavelength of the experiment, heat is deposited only in the interior of the micelles. The use of water droplets suspended in an organic solvent further simplifies the problem since the thermal expansion coefficient of water is so small compared with that of the solvent, the production of the photoacoustic effect through heating and expansion of the micelle itself[11,12] can be neglected. Sound production takes place through conduction of heat from the interior of the micelle to the isooctane, where expansion of the isooctane launches an acoustic wave. The experiments are done using the transient grating technique,[13−21] the time resolution of which is determined by the optical fringe spacing of the grating and the pulse width of the laser. Since the frequency of the acoustic wave is on the order of a few gigahertz, the effects of heat diffusion can be seen from micelles with diameters as small as 10 nm. Because the production of the transient grating depends on the rate of heat diffusion from the micelles into the isooctane, the signal recorded depends on parameters that govern the rate of heat diffusion from the interior of the micelles, namely, the micelle diameter, the ratio of the aqueous phase thermal conductivity to that of the solvent, and thermal diffusivities of the aqueous phase and that of the solvent.

A method for calculation of the transient grating through the photoacoustic effect is given in the Theory section. The properties of the ultrasonic waves are found by first determining the frequency domain temperature profiles of a single droplet surrounded by a heat-conducting liquid. The flow of heat into the solvent is calculated and used together with an expression for the response of a grating to give a Fourier transform integral expression for the time dependence of the grating. The Experiments section describes the apparatus, the experimental procedure, and the reduction of the data. The limitations of the technique are given in the Discussion section.

† Present address: Exxon Chemical Co., Baytown, TX. 77522.

⊗ Abstract published in *Advance ACS Abstracts,* March 15, 1997.

S1089-5647(96)03852-7 CCC: $14.00

Theory of Sound Wave Generation through Heat Diffusion

The characteristics of the photoacoustic effect are governed by the coupled equations for pressure and temperature,[10−22] which, when the effect of viscosity is ignored and the heat capacity ratio γ approximates unity, reduces to the heat equation and a wave equation for pressure. The first of these for a problem of a uniformly heated fluid sphere surrounded by a second fluid can be written as

$$l_h c\,\nabla^2\tau(r,t) - \frac{\partial}{\partial t}\tau(r,t) = -\frac{H(r,t)}{\rho C_p} \tag{1}$$

where τ is the temperature deviation from its ambient value, t is the time, l_h is the characteristic length for heat conduction[22] defined as $l_h = K/\rho C_p c$, where K is the thermal conductivity, ρ is the ambient density, C_p is the specific heat capacity, c is the sound speed, and $H(r,t)$ is the energy per volume and time deposited by the laser at the radial coordinate r, whose origin is taken as the center of the sphere. Fourier transformation of eq 1 gives the ordinary differential equation

$$\nabla^2\tilde{\tau} + k^{t2}\tilde{\tau} = -\tilde{H}(r,\omega)/K \tag{2}$$

k^t is the thermal wavevector defined by

$$k^t = (i\omega/l_h c)^{1/2}$$

where ω is the frequency, and quantities marked with a tilde represent Fourier transforms of time domain quantities with the convention

$$g(r,t) = \int_{\infty}^{-\infty} \tilde{g}(r,\omega)e^{-i\omega t}\,d\omega$$

and

$$\tilde{g}(r,\omega) = \frac{1}{2\pi}\int_{\infty}^{-\infty} g(r,t)e^{i\omega t}\,dt$$

For the present problem the radius of the sphere is taken to be small compared with the wavelength of the exciting radiation so that radiation is absorbed uniformly within the sphere. For delta function heating of a sphere with optical absorption coefficient $\bar{\alpha}$, $H(r,t)$ is given by $H(r,t) = \bar{\alpha}E_0\delta(t)$, the Fourier transform of which is $\tilde{H}(r,\omega) = \bar{\alpha}E_0/2\pi$. The solution to eq 2 must therefore be of the form

$$\tilde{\tau}_s = A[1 + \hat{T}_s j_0(k_s^t r)] \tag{3}$$

$$\tilde{\tau}_f = A\hat{T}_f h_0^{(1)}(k_f^t r) \tag{4}$$

where the frequency domain temperatures inside and outside the sphere are denoted $\tilde{\tau}_s$ and $\tilde{\tau}_f$, respectively, $j_0(z)$ is the zeroth-order spherical Bessel function, $h_0^{(1)}(z)$ is the zeroth-order spherical Hankel function of the first kind, A is an amplitude given by $A = i\bar{\alpha}E_0/\rho_s C_{ps}\omega$, k_s^t and k_f^t are the thermal wavevectors, and $\hat{T}_s$ and $\hat{T}_f$ are complex dimensionless constants. The subscripts s and f throughout the text refer to quantities pertaining to the sphere and the surrounding fluid, respectively.

The amplitude factors are determined by requiring continuity in the temperature and heat flux at the interface between the sphere and the surrounding fluid at $r = a$, which gives $\tilde{\tau}_s = \tilde{\tau}_f$ and $K_s\,\partial\tilde{\tau}_s/\partial r = K_f\,\partial\tilde{\tau}_f/\partial r$. For the present problem, the boundary conditions give two equations that determine T_s and T_f,

$$1 + \hat{T}_s j_0(k_s^t a) = \hat{T}_f h_0^{(1)}(k_f^t a) \tag{5}$$

$$K_s\hat{T}_s k_s^t \left.\frac{\partial j_0(z)}{\partial z}\right|_{z=k_s^t a} = K_f\hat{T}_f k_f^t \left.\frac{\partial h_0^{(1)}(z)}{\partial z}\right|_{z=k_f^t a} \tag{6}$$

where K_s and K_f are the thermal conductivities of the sphere and the surrounding liquid, respectively. Solution of eqs 5 and 6 give the frequency domain temperatures in the sphere and the surrounding fluid as

$$\hat{T}_s = \frac{1 - ik_f^t a}{\left[(\bar{K}-1)\dfrac{\sin k_s^t a}{k_s^t a} - \bar{K}\cos k_s^t a + i\bar{\chi}^{1/2}\sin k_s^t a\right]} \tag{7}$$

$$\hat{T}_f = \frac{i\bar{K}k_f^t a\left[\dfrac{\sin k_s^t a}{k_s^t a} - \cos k_s^t a\right]e^{-ik_f^t a}}{\left[(\bar{K}-1)\dfrac{\sin k_s^t a}{k_s^t a} - \bar{K}\cos k_s^t a + i\bar{\chi}^{1/2}\sin k_s^t a\right]} \tag{8}$$

where $\bar{K}$ and $\bar{\chi}$ are ratios of the thermal conductivities and diffusivities of the material inside the sphere to that outside the sphere, respectively.

In the problem considered here the expansion coefficient of the absorbing sphere is taken to be so small that no photoacoustic effect is generated by heat deposition within its volume. It is only after heat diffusion from the sphere to the surrounding fluid that thermal expansion of the fluid takes place, generating acoustic waves. It is thus only necessary to find the product of the radial heat flux with the area of the sphere multiplied by the number of spheres per unit volume N to give the energy per volume and time delivered to the fluid W. The first of these is found from the radial component of $K_f\nabla\tau_f$, giving the frequency domain heat release function as

$$\tilde{W}(\omega) = -4\pi a^2 NK_f \left.\frac{\partial\tau_f(r,\omega)}{\partial r}\right|_{r=a} \tag{9}$$

Evaluation of the temperature gradient in eq 9 gives $W(\omega)$ as

$$\tilde{W}(\omega) = i4\pi a^3\bar{\alpha}E_0 N\left(\frac{\rho_f C_{pf}}{\rho_s C_{ps}}\right)\hat{T}_f\left[\frac{1 - ik_f^t a}{(k_f^t a)^3}\right]e^{ik_f^t a} \tag{10}$$

which is equivalent to the expression given by Isakovich[24] and that of Zozula and Puchenkov[25] used in their calculation of the properties of the photoacoustic effect generated by a suspension of particles excited by a Gaussian laser beam. Substitution of $\hat{T}_f$ from eq 7 above gives

$$\tilde{W}(\hat{q}) = 4\pi a^3\bar{\alpha}E_0 N\,\frac{(i\hat{q}_f - 1)[\hat{q}_s\cot\hat{q}_s - 1]}{(\hat{q}_s)^2[1 - i\hat{q}_f + \hat{K}(\hat{q}_s\cot\hat{q}_s - 1)]} \tag{11}$$

where the dimensionless frequency parameters for the sphere $\hat{q}_s$ and the suspending fluid $\hat{q}_f$, written in terms of a dimensionless grating parameter $\hat{q}$, have been defined as

$$\hat{q}_s = k_s^t a = ka(1+i)\left(\frac{\hat{q}}{2\hat{l}_{hs}\bar{c}}\right)^{1/2},\quad \hat{q}_f = k_f^t a = ka(1+i)\left(\frac{\hat{q}}{2\hat{l}_{hf}}\right)^{1/2}$$

and

$$\hat{q} = \omega/ck$$

where k is the grating wavevector, $\bar{K}$ is the ratio of the thermal conductivity of the fluid inside the sphere to that of the surrounding fluid, $\bar{c}$ is ratio of the sound speed in the sphere to that in the surrounding fluid, and $\hat{l}_{hs}$ and $\hat{l}_{hf}$ are dimensionless heat conduction parameters defined as $\hat{l}_{hs} = l_{hs}k$ and $\hat{l}_{hf} = l_{hf}k$. The rate at which heat is deposited into the fluid surrounding the spheres governs the generation of the photoacoustic effect, and hence the initial part of the transient grating signal. According to the mathematical development given in ref 10 or 20, the acoustic density can be found by multiplying the frequency domain response of the grating to a delta function heating pulse with the frequency domain heat release function given by eq 11 above and Fourier transforming the result. The time domain density for the transient grating is thus given by

$$\delta(\hat{t}) = \mathrm{i}4\pi a^3 \rho_s \beta \theta_0 N \int_{\infty}^{-\infty} \mathrm{d}q \times \left\{ \frac{\cos \hat{x}}{[\hat{q}^3 + \mathrm{i}\hat{q}^2(\hat{l}'_{vf} + \gamma \hat{l}_{hf}) - \hat{q}(1 + \gamma \hat{l}'_{vf}\hat{l}_{hf}) - \mathrm{i}\hat{l}_{hf}]} \times \frac{(\mathrm{i}\hat{q}_f - 1)[\hat{q}_s \cot \hat{q}_s - 1]}{(\hat{q}_s)^2[1 - \mathrm{i}\hat{q}_f + \bar{K}(\hat{q}_s \cot \hat{q}_s - 1)]} \right\} \mathrm{e}^{-\mathrm{i}q\hat{t}} \quad (12)$$

where θ_0 is the temperature rise of the sphere defined as

$$\theta_0 = \bar{\alpha} E_0 / \rho_s C_{ps}$$

where $\hat{x}$ is a dimensionless coordinate defined by $\hat{x} = kx$, where x is the coordinate along the grating, γ is the heat capacity ratio for the fluid, $\hat{l}'_{vf}$ is the dimensionless viscous length parameter[22] given by $\hat{l}'_{vf} = (\eta + {}^4/_3\mu)k/\rho c_f$, where η and μ are the bulk and shear viscosities of the fluid outside the sphere, and $\hat{t}$ is the dimensionless time given by $\hat{t} = c_f k t$.

For purposes of discussion, eq 12 is written as a product of two factors separated by a "×" sign. The first factor, referred to as the "grating response function", describes the response of the acousic density to a delta function heat deposition, and the second factor, referred to as the "heat release function", is proportional to $\tilde{W}(\omega)$ above and describes the evolution of heat into the region outside the spheres. Note that the expressions for the response of the grating to delta function deposition of heat in refs 10 and 20 are an exact solution to the linearized hydrodynamic equations; thus, eq 12 includes the effects of heat conduction and viscosity in the evolution of the grating after it is launched by heat diffusion from the spheres.

In the reduction of data using Marquard's method, it is necessary to evaluate both $\delta(\hat{t})$ and its derivatives with respect to the parameters θ_0, a, $\bar{K}$, $\bar{\chi}$, $\hat{l}'_{vf}$, and $\hat{l}_{hf}$ many times before the optimized values of the parameters are determined. Numerical evaluation of the Fourier transform integral accurately is difficult owing to the form of the thermal mode described by the integrand;[26] evaluation of the integral in closed form is also difficult because the poles of the second factor in the integrand cannot be found easily. The solution to evaluation of eq 12 taken here is to approximate the second factor in the integrand describing heat release from the sphere with a complex function of the form

$$f(\hat{q}) = \frac{\sum_{n=0}^{n=3} b_{2n}\hat{q}^{2n} + \mathrm{i}\sum_{n=0}^{n=3} b_{2n+1}\hat{q}^{2n+1}}{1 + \sum_{n=1}^{n=3} a_{2n}\hat{q}^{2n} + \mathrm{i}\sum_{n=0}^{n=3} a_{2n+1}\hat{q}^{2n+1}} \quad (13)$$

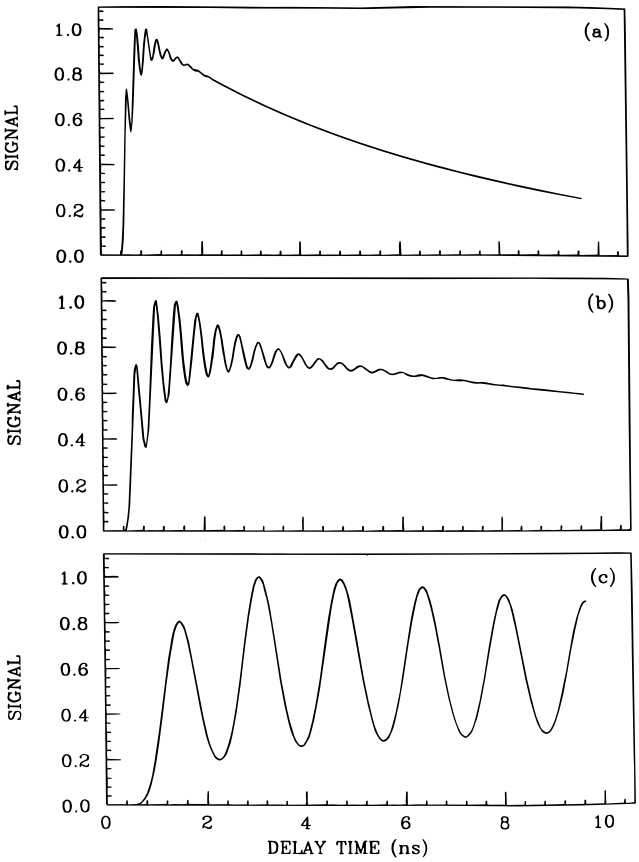

Figure 1. Simulated transient grating signal in arbitrary units calculated from eq 12 versus time in nanoseconds for a suspension of 10.0 nm radius water droplets at grating fringe spacings of (a) 229, (b) 457, and (c) 1828 nm. Other parameters for calculations are $\hat{l}'_{vf} = 0.1$, $\hat{l}_{hf} = 1.24 \times 10^{-3}$, $\hat{l}_{hs} = 1.32 \times 10^{-3}$, $c_f = 1.11 \times 10^3$ m/s, and $\bar{K} = 4.07$. Each curve is normalized to unity. The effect of increasing the fringe spacing to give a larger acoustic period in a−c is to decrease the time for heat release relative to the period of the acoustic wave. The transient grating waveforms show this decrease as a larger acoustic mode (oscillatory) component relative to the thermal mode (exponential decay) component of the signal. In c the time for heat release relative to the acoustic period is so short as to correspond nearly to impulsive launching of the grating, in which case the acoustic and thermal modes initially have identical amplitudes.

where the a's an b's are real quantities. The procedure in calculating $\delta(\hat{t})$ is to assign values of the fitting parameters in the integrand and then to fit $f(\hat{q})$ to the second factor in eq 12 numerically. The roots of the integrand in eq 12 are then found numerically and substituted into the numerator of the integrand. This procedure is based on the assumption that the Fourier transform integral can be evaluated using the residue theorem with a semicircular integration path in the lower half complex $\hat{q}$ plane. Derivatives of $\delta(\hat{t})$ with respect to a given parameter are found numerically by calculating two values of $\delta(\hat{t})$ at two nearby values of the parameter and then dividing by the incremental value of the parameter. An advantage of the approximation method is that it permits an *algebraic* evaluation of $\delta(\hat{t})$: once the poles on the integrand have been found, evaluation of the residues and the integral is straightforward and rapid. The diffracted light signal recorded at the Bragg angle is taken as proportional to the square of the acoustic density. The probe and pump laser pulse widths are convoluted with $\delta(\hat{t})$ in the data-fitting procedure.

The plots in Figure 1 show the effect of changing the grating wavevector on the signal. In each of the plots, the laser pulsewidth is taken to be a delta function in time. Since the diameters of the droplets in the suspension are taken to be

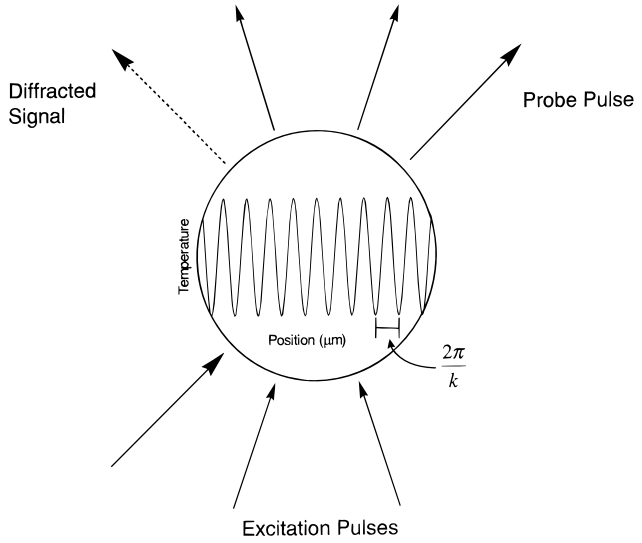

Figure 2. Diagram of the interaction region of the pump and probe beams. The intersection of the two pump beams produces a series of nodes and antinodes in the electric field of the laser beam. Optical excitation of dye molecules in the interior of the micelles followed by nonradiative relaxation of the excited electronic state of the dye and heat diffusion into the fluid surrounding the micelles gives rise to a periodic temperature change in the fluid. This temperature variation, in turn, launches a standing acoustic wave through the mechanism of thermal expansion. Variations in the index of refraction of the fluid arising from the density variations in the fluid diffracts light from the probe beam, the intensity of which is monitored with a photodetector. In the experiments reported here, the fringe spacing of the grating $2\pi/k$ is more than 20 times larger than the micelle diameter.

identical, the time for heat diffusion from the interior of the spheres is the same in each of the plots. Thus, changes in the waveforms seen in the three plots can be attributed to the change in the fringe spacing of the grating. In Figure 1c, the large fringe spacing of the grating and the consequent low frequency of the acoustic wave mean that the shape of the waveform approximates one where heat deposition is nearly instantaneous. The waveform in Figure 1c is to be contrasted with the waveform in Figure 1a, where the grating fringe spacing and acoustic frequency are significantly higher and the heat release time scale is closer to the acoustic period. It follows that experiments done with large grating fringe spacings have a limited ability to resolve the effects of heat release from the spheres on the acoustic waveform and hence to measure the physical parameters governing heat diffusion. Note that in the case of a transient grating the thermal mode of wave motion refers to the change in state variables arising from heat conduction from the antinodal to the nodal regions in the fluid.[22] An obvious feature of the transient grating signals in Figure 1 is that the decay of the thermal mode is more rapid for gratings with small fringe spacings than for gratings with large fringe spacings; the more rapid decay of the former is a straightforward consequence of a larger temperature gradient.

Experiments

The transient grating method, as shown in Figure 2, makes use of the interference of two phase coherent light beams to produce a series of nodes and antinodes of the electromagnetic field in space. At the antinodal points of the field, heat is deposited by the laser in a weakly absorbing fluid; at the nodes of the optical field, no heat is deposited. The periodic deposition of heat in space by short light pulses causes a photoacoustic effect to be generated, launching a standing acoustic wave that is probed by a third laser beam directed at the Bragg angle to the acoustic grating. The salient characteristics of the method are a time response on the order of the acoustic period and response to evolved heat. The transient grating apparatus here used a mode-locked, Nd:YAG laser, Q-switched at 325 Hz to pump two dye lasers.[20] Single pulses from the first dye laser, obtained by cavity dumping, were frequency doubled and split into two equal intensity "pump" beams that were directed into a 1 mm path length cuvette. The energy in the individual pulses at the face of the cuvette containing the micellar solution was typically less than 2 μJ; their pulse widths were 37 ps. The pump beams were focused to a diameter of roughly 400 μm in the cuvette. To subtract out scattered light from the cuvette, one of the two pump beams was alternately switched on and off through use of a chopping wheel synchronized with the laser output. The grating was monitored with the output of the second "probe" dye laser that was time delayed in an optical delay line and then directed into the cuvette at the Bragg angle. The probe beam was focused to a diameter of approximately 250 μm. The diffracted light signal was monitored by a photomultiplier and detected in phase with the chopper by a lock-in amplifier. The lock-in amplifier signal, in turn, was fed to a computer programmed to average the signal over several scans of the delay line. To avoid photochemical bleaching of the dye in the micelles, solutions were alternately pumped into and out of the cuvette via a small reservoir with a reciprocating piston pump.

The reverse micellar solutions were made of the surfactant[27] sodium bis(2-ethylhexyl)sulfosuccinate (AOT), doubly distilled water, and isooctane, which was distilled once before use. The AOT was first added to the isooctane, which was then added to the water as described in ref 29. The solution[27] was stirred for 24 h at which time dye was added. Malachite green or CuEDTA was chosen because of their short radiative lifetimes,[28] their relatively large extinction coefficients, and their low solubility in alkane solvents. The low solubility of these dyes in the isooctane ensured that heat deposition was restricted to the interior of the micelles. The dye concentration was adjusted to give an optical density of 1 mm^{-1} at the pump laser wavelength. It was found that at this optical density the diffracted light signal was large enough to produce a reasonable large signal-to-noise ratio in the averaged signal after 2 h of signal acquisition.

The radii and concentration of the micelles are determined[29,31] by the molar ratio of water to surfactant W, and the volume fraction of water in isooctane ϵ. Thus, it is possible to compare micellar radii found in the experiments here with those from previous light scattering studies of micellar solutions on the basis of the chemical composition of the solutions. For small N, the number density N of micelles in solution is, of course, determined from ϵ through the relation $\epsilon = {}^4/_3\pi a^3 N$.

There was some question as to whether the dye would be uniformly dispersed within the aqueous interior of the micelles or whether it would be concentrated in the AOT near the water−isooctane interface. Although the experiment has no unequivocal means of determining the answer to this question, a simple comparison of the behavior of the two different chromophores in generating transient grating signals was carried out to determine if grossly different waveforms resulted. The experiments were conducted using both the cationic dye malachite green excited at 317 nm at a fringe spacing of 375 nm and the anionic dye CuEDTA excited at 283 nm at a fringe spacing of 464 nm. The resulting two waveforms exhibited slightly different shapes that could be primarily attributed to the different fringe spacings employed.

Typical experimental data where CuEDTA was used as the chromophore are shown in Figure 3. The plots in Figure 3a−c

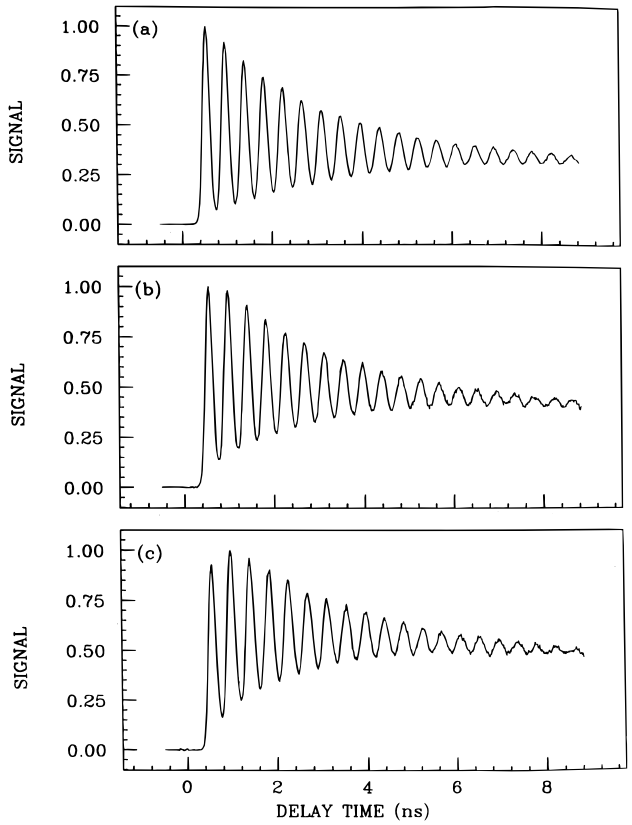

Figure 3. Transient grating signal in arbitrary units versus time in nanoseconds for AOT/water/isooctane reverse micellar solutions with micelle radii (a) 3.5 nm ($W = 10$, $\epsilon = 0.035$), (b) 7.5 nm ($W = 30$, $\epsilon = 0.11$), and (c) 17 nm ($W = 60$, $\epsilon = 0.21$). The excitation wavelength was 283 nm, and the grating fringe spacing was 464 nm. Each of the curves was normalized to unity.

are experimental transient grating signals for three different size micelles. The data in Figure 3a are from a micellar solution where the rate of heat release from the micelles is so rapid compared with the period of the acoustic wave that the launching of the photoacoustic wave can be considered as arising from an instantaneous source: the heat release, insofar as the transient grating is concerned, is so rapid that the photoacoustic effect is generated as if it were from a dye solution where the molecules are uniformly dispersed in solution. No attempt to extract information concerning the diameter or thermal properties of the micelles from such data was made. Data in Figures 3b,c, on the other hand, show the slow rise in the thermal mode and the reduced amplitude of the acoustic mode expected when there is a gradual release of heat from the somewhat larger micelles.

Next, a series of experiments were carried out to determine whether the thermal method could be used as a method of measuring micellar radii. Data similar to those in Figures 3b,c but taken with an excitation wavelength of 283 nm and an optical fringe spacing of 876 nm were fit using Marquardt's method with six adjustable parameters: the signal amplitude, the probe beam delay time relative to the time of firing of the pump laser, c_f, $\hat{\Gamma}_{vf}$, $\hat{\Gamma}_{hf}$, and the micellar radius a. Values of the thermal diffusivities and conductivities for water and isooctane were taken from ref 32. The best fit values from Marquardt's method for the micelle radius, denoted a_{th} for the thermal diffusion method, are shown in Table 1 along with the results of light scattering measurements on the solutions, denoted a_{ls}, and results taken from ref 29, denoted a_{ref}, where solutions with identical chemical compositions were assumed to give identical size micelles. Note that the radii reported in ref 29 were determined using dynamic light scattering. The disagreement in Table 1 between the two light scattering measurements at $W = 60$ and $W = 80$ is substantial, but can almost certainly be attributed to slight differences in the composition or method of preparation of the solutions. No measurements at $W = 100$ were reported in ref 29. From Table 1 it can be seen that the mean values of the radii increase with increasing W so that the thermal diffusion method of determining micellar radii gives the expected trend of larger micellar radii as W increases. However, the errors in the measurements show that values for the radii overlap for successive W values. The agreement between the thermal diffusion and light scattering determinations of the micellar radii is excellent. The agreement is quite fortuitous however since determinations of a_{th} from experiments using a smaller fringe spacing of 458 nm give radii nearly a factor of 2 smaller than those reported in Table 1 obtained at a fringe spacing of 876 nm. The origin of the sensitivity of a_{th} to the grating wavevector is not clear. The best fit radii shift comparably, maintaining qualitatively correct relative radii for different micelles.

TABLE 1: Comparison of Experimentally Determined Micellar Radii

W	a_{th} (nm)	a_{ls} (nm)	a_{ref} (nm)
60	11 ± 2	10.3	17.0
80	12 ± 4	12.4	29.0
100	15 ± 1	15.0	

Discussion

It is clear from eq 10 or 12 that three heat diffusion parameters, the droplet radius, its thermal diffusivity, and the heat conductivity ratio, determine the rate at which heat leaves the micelle. These three parameters thus govern the time evolution of the photoacoustic effect, and hence the shape of the initial part of the transient grating waveform. It is straightforward to calculate waveforms for various values of the these three parameters using eq 12 and to see the effect of changes in the parameters on the waveforms. The extraction of the three parameters in a data-fitting procedure, on the other hand, is a far more complicated problem than calculation of waveforms since, in the case of the present problem, a variation in the shape of the measured waveform does not necessarily result in unique changes in the three heat diffusion parameters.

The reason for the difficulty in fitting of the three thermal parameters can be illustrated by a plot of the real parts of the two factors in the integrand of eq 12, as shown in Figure 4. The magnitude of the first factor in eq 12, which represents the response of the density to instantaneous heat deposition, is plotted against the frequency parameter in Figure 4a. The peak at $\hat{q} = 0$ corresponds to the thermal mode that describes the density change when heat is slowly conducted from the antinodal to the nodal regions of the grating. The peak at $\hat{q} = 1$ or, equivalently, at $\omega = ck$ describes the acoustic mode, with the position of the peak determining the frequency of the density oscillation and the width of the peak giving the damping. For the problem of heat diffusion from a sphere, the grating response must be multiplied by the heat release function plotted in Figure 4b. If the two curves are multiplied together, it can be seen that owing to the smoothness of the factor describing heat release, the effect of the multiplication, especially when the peaks in the grating response curve are sharp, is primarily to modify the amplitudes of the thermal and acoustic modes. Note also that the overall amplitude is not an experimentally determined parameter that is fitted to eq 12; only the relative amplitudes of the two peaks is of importance. Now, changes in any of the three thermal parameters result in a somewhat

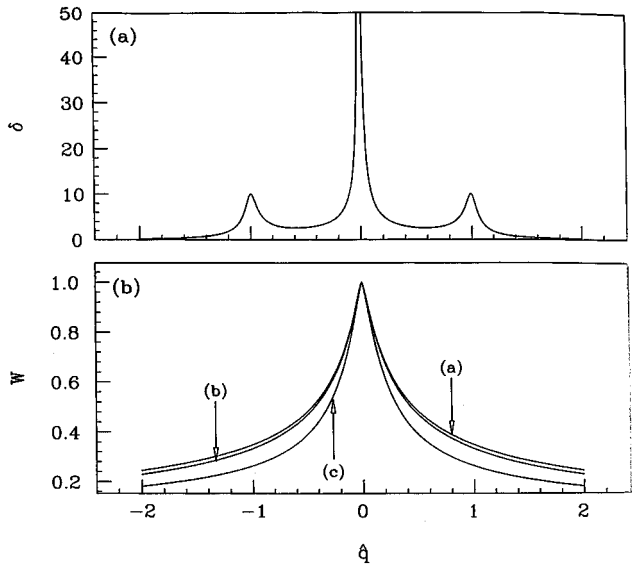

Figure 4. (a) Magnitude of the grating response function in arbitrary units versus the frequency parameter $\hat{q}$. (b) The magnitude of the heat release function in arbitrary units versus $\hat{q}$ from the integrand of eq 12. The three curves are plotted for (a) $\bar{K} = 8.0$, (b) $\bar{K} = 4.07$, corresponding to water surrounded by isooctane, and (c) $\bar{K} = 1.0$.

different shape in the heat release curve. However, if it is only the relative amplitude of the two peaks in the integrand of eq 12 that is modified, then the shape of the heat release function is not important. Equivalently, it can be said that the character of the heat release curve is modified by the thermal parameters, but the process of its multiplication by the grating response curve erases that character. In essence, only the relative amplitudes of the thermal and acoustic modes are modified by the process of heat diffusion: to a large extent, the three thermal parameters act equivalently. The loss of information in the heat release function shows up in parameter-fitting algorithms as a flat surface in a plot of the error squared versus fitting parameters: any number of values for the fitted parameters can be used to give the same value of squared error. In fact, the integrand in eq 12 is the product of two complex factors. The acoustic density, on the other hand, is purely real and has contributions from both the real and imaginary parts of the grating response and heat release functions. A plot of the imaginary part of the former shows that it too is a peaked curve, with a central peak and peaks at $\hat{q} = \pm 1$ resembling the derivative of those at $\hat{q} = \pm 1$ in Figure 4a. The difficulty in preserving the dependence on all three heat diffusion parameters when only a small region of the curve is sampled by the grating response function is the same as the one-dimensional example illustrated in Figure 4. A quantitative discussion of this point would, of course, involve calculation of the derivatives of the acoustic density with respect to each of the fitting parameters.

The procedure used here is to take the values of the thermal diffusivity and thermal conductivity as known quantities and to fit the data to a single parameter, the micellar radius. A single-parameter fit should not be problematic since the relative amplitudes of the peaks at $\hat{q} = \pm 1$ and $\hat{q} = 0$ govern the amplitudes of the acoustic and thermal modes, as is clearly evident from inspection of Figure 4. It is, of course, entirely possible to take the micellar radius as a known quantity, as for instance from a light scattering measurement, to pick one of $\bar{\chi}$ or $\bar{K}$, and to fit the data to the other. In fact, given that measurements of hydrodynamic radii by dynamic light scattering are carried out routinely, determination of $\bar{\chi}$ or $\bar{K}$ may prove to be the more interesting quantity, especially in light of the well-known entropy effect in micellar solutions where ordered structure in the vicinity of the surfactant molecules has been inferred.[34] However, since the point of the present study has been to investigate the feasibility of the thermal diffusion technique, the micellar radius was fit rather than one of the other parameters so that a comparison with light scattering measurements would be possible.

The origin of the effect where larger micelle radii are found at larger optical fringe spacings is not certain. Clearly, the experiments reported here do not definitively answer the question of whether or not the dye is uniformly dispersed within the micelle. If the dye has a concentration at the perimeter of the micelle that is higher than that at its center owing to the presence of the surfactant molecules, then the heat release curve will have more high-frequency components than would be predicted by the above uniform heat deposition model. Since experiments conducted with small fringe spacings respond preferentially to the high-frequency components in the heat release curve, as is evident from Figure 4, the effect of such a nonuniform heat distribution would be to give an apparent smaller micellar radius at small fringe spacings, but not so at large fringe spacings. Experiments to measure the effect of nonuniform dye distributions are in progress.

In conclusion it can be said that the thermal diffusion method introduced here offers the possibility of a new method of determining heat diffusion parameters for micellar solutions, emulsions, and suspensions of solid particles. Clearly, the thermal diffusion method is qualitatively different from neutron and dynamic light scattering, which are the most commonly used methods for determination of particle diameters; the unique ability of the thermal method to determine thermal diffusion parameters as shown in the Theory section and the ease with which transient grating data in micellar solutions can be generated suggest further investigation of the method despite the difficulties in data reduction reported here.

Acknowledgment. The authors are grateful for support of this research by the U.S. Department of Energy, Office of Basic Energy Studies, under Grant ER13235. M.B.Z. gratefully acknowledges support from the National Science Foundation under Grant CHE-9206765.

References and Notes

(1) Sigrist, M. W. In *Air Monitoring by Spectroscopic Techniques*; Sigrist, M. W. Ed.; John Wiley: New York, 1994.

(2) Gusev, V. E.; Karabutov, A. A. *Lazernaya Optoakustika*; Naoka: Moscow, 1991; English translation *Laser Optoacoustics*; AIP Press: New York, 1993.

(3) *Lasers in Acoustics*; Bunkin, F. V.; Kolomensky, A. A.; Mikhalevich V. G. Eds.; Harwood Academic Publishers: Reading, MA, 1991.

(4) Egerev, S. V.; Lyamshev, L. M.; Puchenkov, O. V. *Usp. Fiz. Nauk* **1990**, *160*, 111 [*Sov. Phys. Usp.* **1990**, *33*, 739.

(5) Tam, A. C. *Rev. Mod Phys.* **1986**, *58*, 381.

(6) Patel, C. K. N.; Tam, A. C. *Rev. Mod. Phys.* **1981**, *53*, 517.

(7) Lyamshev, L. M. *Usp. Fiz. Nauk* **1981**, *135* 977; [*Sov. Phys. Usp* **1981**, *24*, 977].

(8) Lyamshev, L. M.; Sedov, L. V. *Akust. Zh.* **1981**, *27*, 5; [*Sov. Phys. Acoust* **1981**, *27*, 4.

(9) This statement has been investigated only in the case where the absorbing body and the surrounding fluid have the same properties. See: Cao, Y. N.; Diebold, G. J. *Opt. Eng*., in press.

(10) Chen, H. X.; Diebold, G. J. *J. Chem. Phys.* **1996**, *104*, 6730.

(11) Diebold, G. J.; Westervelt, P. J.; J. *Acoust. Soc. Am.* **1988**, *84*, 2245. This paper has the following tpyographical errors. A factor of $\hat{r}$ is missing in eq 6: the numerator should have the factor (sin $q\hat{r}$/$q\hat{r}$). Equation 17 is missing a minus sign. After eq 30, T reduces to $2/(1 + c_s/c_f)$. Before eq 33, the effective mass should be $4\pi a^3\rho_f$. The phase lag curves in Figures 2 and 3 are missing changes where the amplitude is zero.

(12) Diebold, G. J.; Khan, M. I.; Park, S. M. *Science* **1990**, *250*, 101.

(13) Eichler, H. J.; Gunter, P.; Pohl, D. W. *Laser-Induced Dynamic Gratings*; (Springer-Verlag: Berlin, 1985.

(14) Nelson, K. A.; Dwayne Miller, R. J.; Lutz, D. R.; Fayer, M. D. *J. Appl. Phys.* **1982**, *53*, 1144.

(15) Miller R. J. D. In *Time Resolved Spectroscopy*, Clark, R. J. H.; Hester, R. E., Eds.; John Wiley: New York, 1989.
(16) McGraw, D. J.; Harris, J. M. *Opt. Lett*. **1985**, *10*, 140.
(17) Fayer, M. D. *IEEE J. Quantum Electron*. **1986**, *22*, 1437.
(18) Terazima, M.; Hirota, N. *J. Chem. Phys*. **1991**, *95*, 7490.
(19) Duggal, A. R.; Nelson, K. A. *J. Chem. Phys*. **1991**, *94*, 7677.
(20) Sun, T.; Morais, J.; Diebold, G. J.; Zimmt, M. B. *J. Chem. Phys*. **1992**, *97*, 9324. For the present calculation, eq 17 of this reference should be normalized by dividing out the frequency domain response of the delta function before multiplying by $\tilde{W}(\omega)$.
(21) Khan, M. I.; Goodman, J. L. *J. Am Chem. Soc*. **1995**, *117*, 6635.
(22) Morse, P.; Ingard, K. U. *Theoretical Acoustics*; McGraw-Hill: New York, 1968. See, in particular, section 6.4.
(23) McGraw, D. J.; Harris, J. M. *Phys. Rev.* **1986**, *A34*, 4829.
(24) Isakovich, M. A. *Zh. Eksp. Teor. Viz*. **1948**, *18*, 907.
(25) Zozula, O. M.; Puchenkov, O. V. *Akust. Zh*. **1993**, *39*, 92−100; [Eng.transl. *Acoust. Phys*. **1993**, *39*, 46−50. The complex conjugate of their $h(\omega)$ is proportional to our $\tilde{W}(\omega)$.
(26) Walker, James S. *Fast Fourier Transforms*; CRC Press: Boca Raton, 1991.
(27) The AOT was supplied by Aldrich Chemical Co. and used without further purification. The CuEDTA was synthesized by mixing $Cu(OH)_2$ with an equimolar amount of EDTA in a pH ≅ 9 NaOH solution then filtering the resulting solution.
(28) Ben-Amotz, D.; Harris, C. B. *J. Chem. Phys*. **1987**, *86*, 4856.
(29) Zulauf, M.; Eicke, H. F. *J. Phys. Chem*. **1979**, *83*, 480.
(30) Eicke, H. F. In *Microemulsions*; Robb, I. D., Ed.; Plenum: New York, 1982.
(31) Langevin, D. In *Structure and Reactivity in Reverse Micelles*; Pileni, M. P., Ed.; Elsevier Science: New York, 1989.
(32) *The Chemical Rubber Company Handbook*; CRC Press: Boca Raton, 1992.
(33) The dynamic light scattering experimets were done at Exxon Research Laoratories, Annandale, NJ.
(34) Tanford, C. *The Hydrophobic Effect*; John Wiley and Sons: New York, 1973.